

UNIVERSITÄT LEIPZIG

LEIPZIGER INSTITUT FÜR METEOROLOGIE

**Long-Term Trends in  
Mesospheric Winds and gravity  
waves extracted from meteor  
radar measurements and GAIA  
simulations**

Jason Müller  
22. September 2020

## Contents

<b>1</b>	<b>Introduction</b>	<b>2</b>
1.1	Some basic theory . . . . .	3
<b>2</b>	<b>Data</b>	<b>4</b>
2.1	Meteor radars . . . . .	4
2.2	Ground-to-topside model of Atmosphere and Ionosphere for Aeronomy (GAIA) . . . . .	5
<b>3</b>	<b>Methodology</b>	<b>6</b>
<b>4</b>	<b>Results</b>	<b>6</b>
4.1	Kiruna 67° N, 20° O . . . . .	6
4.2	Collm 52° N, 15° O . . . . .	7
4.3	Tavistock 43° N, 81° W . . . . .	7
4.4	Rio Grande 53° S, 67° W . . . . .	8
4.5	Davis-Station 68° S, 77° O . . . . .	9
<b>5</b>	<b>Discussion</b>	<b>9</b>
5.1	The stations . . . . .	9
5.2	Comparison to Wilhelm et al. (2019) . . . . .	10
5.2.1	Comparing Andenes to Kiruna . . . . .	10
5.2.2	Comparing Juliusruh to Collm . . . . .	11
<b>6</b>	<b>Conclusion</b>	<b>11</b>

## Abstract

This text aims to present the main findings of a student project which is part of the course "Upper Atmosphere" 2020 at the Leipzig Institute for Meteorology. The project's main goal was to investigate the long-term trends in the wind field and the Gravity-inertia-wave (GWs) activity in the Mesosphere and lower Thermosphere. The data was extracted from meteor-radars at five different Stations: Kiruna, Collm, Tavistock, Rio Grande and Davis-Station, between 1999 and 2019. Additionally, the data was later compared to GAIA-model simulations. The results suggest a highly variable wind field with a strong seasonal pattern. At many stations, strong and significant trends were observed, however the sign, the magnitude and the time of year and altitude differs widely between the stations. Some significant trends were found to be linked to trends in GW activity, for others, no connection was found. In general, trends in the meridional wind component and in lower latitudes were more often linked to trends in GW activity than trends in the zonal wind component and in higher latitudes. The performance of the GAIA-model in simulating both climatologies and long-term trends depends on the station. By far the best performance was observed over Davis. The results were also compared to the findings of Wilhelm et al. (2019), where a reasonable accordance was found.

## 1 Introduction

Concerns that the anthropogenic-induced climate change might not only affect the Troposphere, but might also have an impact on the upper atmosphere were already raised in the early 1990s for example by Rind and Lacis (1993). Thomas (1996) investigated specifically the possible trends in the Mesosphere and lower Thermosphere (MLT) using simple models. Since then, many more studies investigated the dynamics and trends in this atmospheric region, using many different measurements. Most studies relied on either ground-based or space-born remote sensing techniques such as Lidars, passive radiometers and radars (Wilhelm et al., 2019). However, as Jacobi et al. (2005) point out, most of the conducted measurements are temporally limited and rely on only few stations.

Portnyagin et al. (2006) analysed three mid-latitudes stations in Collm (Germany), Odninsk (Russia) and Saskatoon (Canada) from 1964 to 2004. They found a significant trend in the zonal (meridional) wind but only until the 1980s (1990s). However, they found more trends in seasonal data and concluded that even longer time series would be necessary to detect possible trends in the overall wind field. Since the time series used here are even shorter, this project will be focused on trends in single months rather than overall trends.

Baumgaertner et al. (2005) for example used a medium frequency radar to investigate long-term trends over Scott Base in Antarctica. They did not find any significant trends in the mean zonal or meridional winds. However, they found cycles, as well as trends in the different tides and planetary waves. They also found hints towards an influence of the solar cycle on different tides. They too stress that, because of the large inter-annual variability of some of the measured parameters, longer time series are essential for assessing long-term trends in the MLT.

Wilhelm et al. (2019) used meteor radar measurements to investigate the long-term changes in three stations: Andenes, Juliusruh and the CMA station in Tavistock, Ontario. They found a clear dependence of the climatologies on the latitude for the zonal and meridional wind. They also found strong and significant trends in the winds for specific months, while the overall wind only showed weak trends. The observed linear monthly trends depend on the station, the altitude and the time of the year. The significance of the trends also highly depends on the observed time frame. Besides that, they too found an impact of the solar cycle on different tidal modes, planetary waves and on the mean wind.

This project aims to extend the efforts of Wilhelm et al. (2019) and many earlier studies and, evaluate long-term trends of the wind in five stations, namely: Kiruna ( $67^{\circ}$  N  $20^{\circ}$  O), Collm ( $52^{\circ}$  N,  $15^{\circ}$  O), (again) Tavistock ( $43^{\circ}$  N,  $81^{\circ}$  W), Rio Grande ( $53^{\circ}$  S,  $67^{\circ}$  W) and Davis-Station ( $68^{\circ}$  S,  $77^{\circ}$  O).

This project is focused on the altitudes between 72 km and 102 km. This region is commonly considered as part of the Mesosphere-and-lower-Thermosphere (MLT), although the definition of this region depends on the literature, e.g. 50-100 km in Thomas (1996) and 70-110 km in (Jacobi et al., 2001).

Although this region only contains only about 0.1% of the mass of the atmosphere, investigating it might be important for various reasons(Thomas, 1996). The MLT seems to be sensitive to changes in the tropospheric climate, and could therefore be used as a tool to evaluate climate models as a early warning sign if major trends are measured. Besides that, trends in the MLT might also have a direct effect on the radiation budget. Furthermore, the middle atmosphere is also coupled downward to the lower atmosphere by dynamical and radiative processes (Holton, 2012).

## 1.1 Some basic theory

The dynamics of the MLT are in many ways different from the tropospheric dynamics. Andrews et al. (1987) describe all major processes of not only the MLT but the whole middle atmosphere in great detail and with some mathematical background. The following brief description of the general circulation patterns and their driving forces is based on Andrews et al. (1987) and Holton (2012).

The MLT can be considered as the top of the middle atmosphere. Within in the MLT, there is a change of sign in the vertical temperature gradient from negative in the Mesosphere to positive in the Thermosphere. The height of this transition varies in time and latitude and is called Mesopause. The MLT is also right below the so called Homopause, where molecular diffusion starts to dominate above turbulent mixing due to decreasing density. It is therefore noteworthy that the atmosphere can still be regarded as mostly well mixed in and below the MLT, but not above. Lastly, it is important to note that the background air in the MLT is mostly neutral, which is again not the case in higher altitudes.

The dynamics in the MLT are mostly driven by four components: (1) The radiative heating and cooling, especially by ozone, (2) Tidal waves, (3) Planetary waves, and (4) Gravity-Inertia-Waves (GWs). Tidal waves mainly have a short-term influence on the wind-field and thus will not be analysed during this project. However, long-term changes in tidal waves are likely to also cause trends in the wind-field. Also, planetary wave activity will not be considered here.

However, the GW activity is a key part of this project. GWs are mainly produced in the Troposphere by many different processes, as summarized by Fritts and Alexander (2003). Some, but not all phenomena that lead to a GW production are: convection, wind shear or topographical forcing, e.g., the flow over mountains.

The resulting gravity waves are controlled by the gravity force on the one hand and their own inertia on the other. Propagating upwards, they carry along a specific momentum with a zonal and meridional component. As the density decreases exponentially, energy conservation lets the amplitude of the waves increase exponentially with height. When the amplitude becomes too large, the wave becomes unstable and breaks, depositing its momentum onto the background winds. This can either further accelerate or drag the background wind, depending on the sign of the carried momentum and the background wind. This process is highly complex and again explained in great detail and with a mathematical derivation by Andrews et al. (1987). GWs can also get filtered when their phase speed matches the background wind speed in direction and amplitude. In this situation, the GW cannot propagate through the atmospheric layer and will again deposit it's momentum onto the background circulation. In the MLT, both effects, breaking and filtering, occur frequently and thus, GW-momentum-deposition is believed to play a major role in the MLT-circulation (Holton, 2012).

The following very brief summary of the zonal-mean circulation is again based on the works of Andrews et al. (1987). The zonal-mean zonal flow is shown in figure 1 where the situation for solstice is displayed. Besides the two tropospheric, eastward jets, the figure also shows two jet streams in the middle-atmosphere. The middle-atmospheric jet in the winter hemisphere is westerly (flows eastward) and reaches up to over 100 km altitude. The jetstream in the summer hemisphere is directed towards the east, but slows down in lower altitudes until there is a wind reversal in roughly 90 km height. Above that, the wind is westerly. This slowing of the wind as well as the reversal are commonly associated with the momentum deposition of breaking GWs. As it is pointed out by Andrews et al. (1987), this is not to be mistaken for a genuine climatology as there are hemispheric differences. Besides that, for example Jacobi et al. (2012) also showed that the wind field can also differ between different longitudes.

While the undisturbed circulation would be just zonal, the impact of GWs, tides and planetary waves also drives a meridional circulation. For a figure of the meridional circulation see e.g. Holton (2012). This secondary, wave-driven circulation is always directed towards the winter pole, i.e., northwards in the northern-hemisphere-winter and vice versa. For continuity reasons, this intensive meridional flow triggers an ascending motion over the summer pole and a descending motion above the winter pole. Adiabatic heating (and cooling) then leads to an inversed temperature structure, where the MLT-summer pole is up to 60 K colder than the winter pole. These extremely low temperatures above the summer pole then lead to phenomena like Noctilucent Clouds (Dowdy et al., 2007).

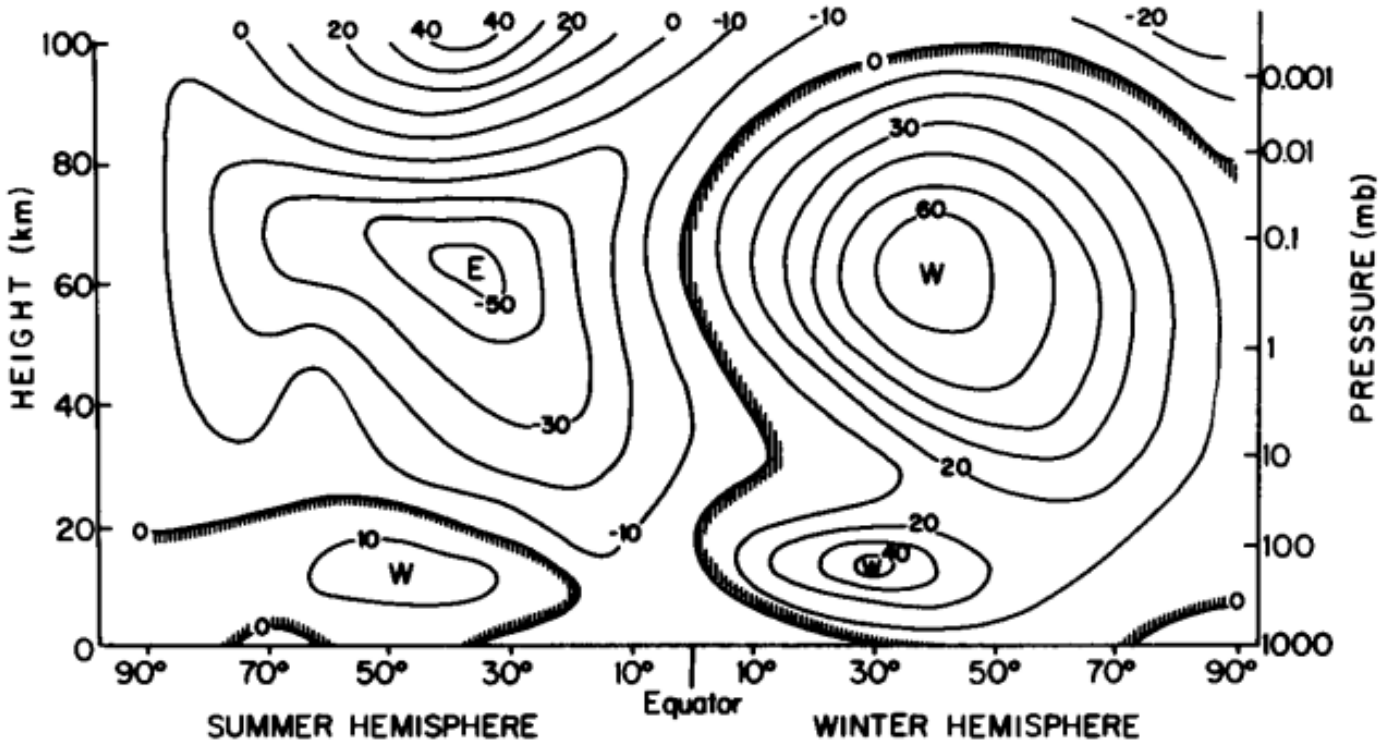


Figure 1: Schematic zonal wind by Andrews et al. (1987)

## 2 Data

### 2.1 Meteor radars

Meteor radars are located at each of the five stations. For a detailed description of the functionality of a meteor radar, see, for example Palo (2007).

Meteoroids enter earth's atmosphere usually with extremely high speeds, up to  $72 \text{ km h}^{-1}$ . This large amount of kinetic energy is transformed to heat due to friction when the meteors enter atmospheric layers with higher density, leading to an evaporation of the meteor. The gas left behind is highly ionized by the extreme temperatures. This process mainly takes place in the layer roughly between 70 km to 130 km, which happens to be the MLT, the layer of interest for this project. This trail of ionized gas reflects radar signals, in contrast to the neutral background atmosphere. These are the radar signals measured by meteor radars. By analyzing the Doppler-shift of the reflected signal or directly projecting the measured radial movement of the trail on the background wind, the horizontal wind speed can be derived (Wilhelm et al., 2017). As a result, the quality of the data is highly dependent on the number of measurable meteors. For that reason the radar data used for this project are limited to heights between 72 km and 102 km to avoid bias due to missing data. Possible outliers on the upper or lower edge of the frame are likely due to this effect and should not be considered for further analysis.

Typical frequencies used for meteor radars reach from 10 to 50 MHz. The exact frequencies and powers of the radar vary and are not provided here.

The five stations used for this project are shown in figure 2. Two of the stations (Rio Grande and Davis) are on the southern hemisphere, while Kiruna, Collm and Tavistock are on the northern hemisphere. While no tropical stations are considered, Davis and Kiruna are located in the high latitudes. The others can be regarded as mid-latitude stations. The data availability for the different stations can be seen in table 1. As already pointed out in section 1, a long time series is crucial for reliable results. The length of the available data reaches from 22 years in Kiruna to only 11 years in Rio Grande, which is only one solar cycle and might therefore be biased and easily influenced by outliers. This must be kept in mind during the analysis.

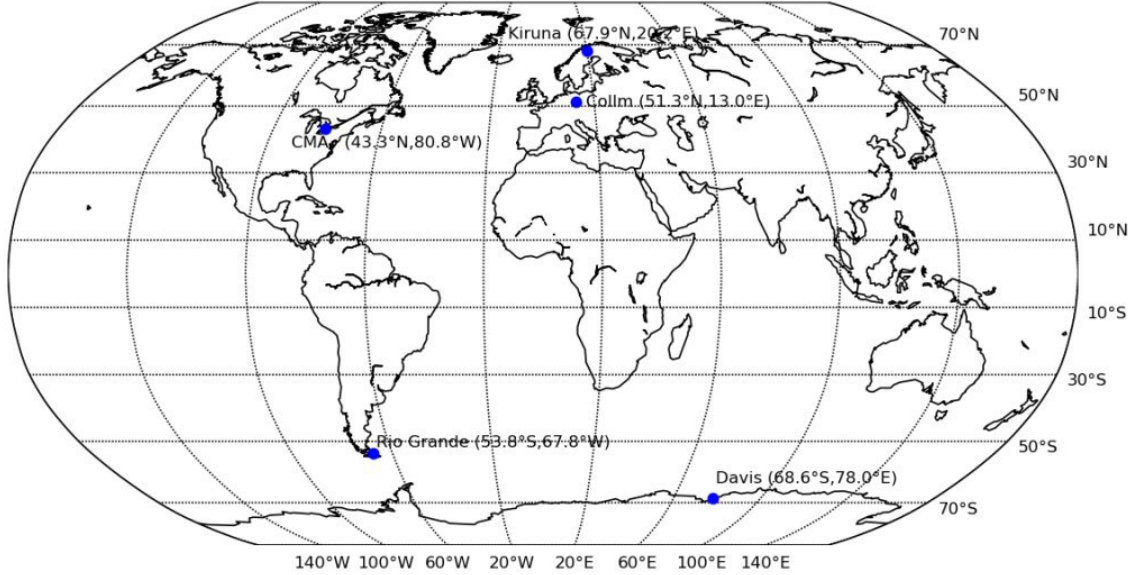


Figure 2: Map of the five considered stations with latitude and longitude; by BENEDIKT GAST.

Table 1: Start and end times of the time series from the meteor radars and the GAIA simulations

Station	Meteor radar		GAIA	
	Start	End	Start	End
Kiruna	01.08.1999	31.12.2019	01.08.1999	31.12.2017
Collm	01.08.2004	06.03.2019	01.08.2004	31.12.2017
Tavistock	01.01.2002	31.12.2018	01.01.2002	31.12.2017
Rio Grande	01.02.2008	31.12.2019	01.02.2008	31.12.2014
Davis-Station	01.01.2005	31.12.2019	01.01.2005	31.12.2017

## 2.2 Ground-to-topside model of Atmosphere and Ionosphere for Aeronomy (GAIA)

The results gathered from the meteor radar measurements are compared to the results of GAIA simulation runs, carried out for similar time frames.

The Ground-to-topside model of Atmosphere and Ionosphere for Aeronomy (GAIA) is a model that simulates the whole atmosphere. In order to simulate the atmospheric system as a whole, it features three sub-models: The atmospheric model deals with the neutral region of the atmosphere up to the Thermosphere from 0 to 600 km. It simulates meteorological processes, photochemical reactions, and wave propagation. Vertical coupling is self-coherently simulated within the neutral atmosphere as well as between neutral atmosphere and Ionosphere. The atmospheric model runs with a spatial resolution of 1.125° to 5.6° in the horizontal direction and between 0.2 to 0.4 scale heights in the vertical dimension.

The Ionospheric model simulates the dynamics of the plasma in the atmosphere between 100 and 3000 km. It also features photochemical reactions of different ions such as O<sup>+</sup>, O<sub>2</sub><sup>+</sup>, N<sub>2</sub><sup>+</sup> and NO<sup>+</sup>. For that, a resolution of 5° x 1° to 1° x 1° is used. The vertical resolution is at least 10 km.

Lastly, the Electrodynamics model runs simulations for the ionospheric currents and electric fields that are produced by flowing charged particles. The resolution is not fixed and is dependent on the outcome of the other two components.

Coupled together, the sub-models calculate a self-consistent simulation for the whole atmosphere. However, there are weaknesses, e.g., in the structure of the model geomagnetic field or the solar irradiance inputs.

For more detailed information about the concepts, functionality, limits and perks of GAIA, the official website

of the GAIA project<sup>1</sup> or the presentation by Huixin Liu; Kyushu University, Japan<sup>2</sup>, can be consulted. These were also the sources for this section.

The start and end times for the simulation runs for the different stations are also shown in table 1. They roughly match with the time frames of the corresponding measurements.

### 3 Methodology

An adaptive spectral filtering was applied to the original radar and model data. This allows a splitting of the wind data into daily mean wind, different periods of tides and a residual wind which contains some left tide components, but most importantly: GWs. The aim of this is to filter out regular phenomena with small time scales. Wilhelm et al. (2019) used the same technique and the details of the procedure are deeper explained in their paper.

To assess the GW activity, the residual wind extracted from the adaptive spectral filtering was analysed. For that, the different pre-calculated tides were subtracted from the mean wind to obtain a residual wind. The residual wind contains GWs. To obtain information about the GW activity, the (specific) GW kinetic energy  $E$  is calculated before averaging. The GW kinetic energy is defined here as  $E = \frac{1}{2}(u^2 + v^2)$  (Geller and Gong, 2010).

The data was evaluated in 2 km steps in altitude. To produce the climatologies, all available data for every station was averaged weekly to exclude phenomena with small timescales but still obtain a fairly high resolution.

To evaluate the long-term changes, a linear trend was calculated. The code is provided on [https://github.com/VACILT/trends\\_project](https://github.com/VACILT/trends_project). This was done by applying a linear least-squares regression on the monthly averaged data. The monthly mean was used here in an attempt to obtain more reliable and robust trends. In addition, a hypothesis test (Wald Test with t-distribution) was performed on the linear regression to evaluate the significance of the trends. The Null hypothesis for this test was that there is in fact no linear trend. The p-values can be thought of as the probability of obtaining the calculated trend randomly if there is no real trend. In this project, trends with p-values under 0.05 (0.01) are regarded as significant. Further information on the statistics-function used to calculate the trends and the p-values can be found in the online-documentation: <sup>3</sup>

The summer and winter solstices are marked in the plots as an orange vertical line. Note that a purely solar-driven atmosphere would be symmetric around this lines with only slight deviations due to thermal inertia.

## 4 Results

The following section presents a collection of the most striking features which came up during the project.

### 4.1 Kiruna 67° N, 20° O

Figure 3 shows the measured and simulated climatologies for the zonal and meridional wind in Kiruna. The measured zonal wind (figure 3a) is in good agreement with the theory described in section 1.1. During winter time, positive (eastward) winds dominate with a maximum in wind speed in February below 80 km altitude. The transition between winter and summer circulation occurs in March, where there is no weekly-mean zonal wind at all. After that, the summer circulation develops a westward wind in all heights for a short period of time. As it is described in the theory section, the subsequent wind reversal again directs the flow into an eastward direction above 90 km. The weekly-mean zonal winds in summer are genuinely stronger than in winter.

The simulated zonal wind (figure 3c) reproduces the basic circulation pattern. However, it fails to simulate the summer wind-reversal, commonly associated with GW activity (see section 1.1). Instead, it simulates a westward maximum in total wind speed in spring which cannot be seen in the measured data. Instead of positive wind speeds in the region of the wind reversal, the simulations at least show a reduction of the total wind speed.

The situation for the measured meridional (figure 3b) and for the simulated meridional (figure 3d) wind is similar to the zonal component. While the overall structure is the same some details are different. The most striking difference is the magnitude of the summer and winter winds. While the observations show a maximum in

<sup>1</sup>Official website: [https://gaia-web.nict.go.jp/models\\_e.html](https://gaia-web.nict.go.jp/models_e.html)

<sup>2</sup>Presentation: [https://www.dropbox.com/s/sxaem3cl9vykpis/Huixin\\_IAP2019.pdf?dl=0](https://www.dropbox.com/s/sxaem3cl9vykpis/Huixin_IAP2019.pdf?dl=0)

<sup>3</sup><https://docs.scipy.org/doc/scipy/reference/generated/scipy.stats.linregress.html>

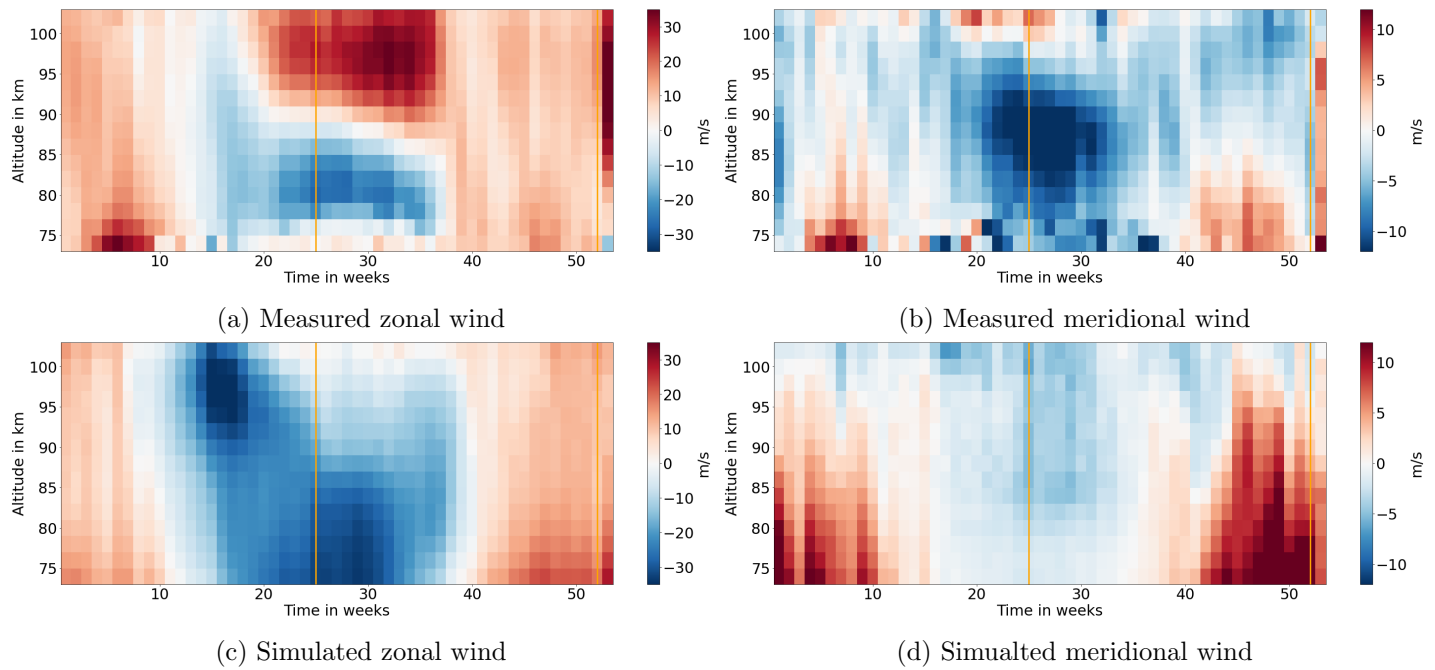


Figure 3: Weekly averaged zonal and meridional wind climatologies for Kiruna. As in all the following figures, the orange vertical lines mark the summer and winter solstice.

total wind speed in the summer-southward winds, GAIA simulates the greatest wind speeds during the winterly-northward winds.

Neither the observation nor GAIA shows significant trends worth mentioning in Kiruna. Therefore, these pieces of information are not provided here. The few significant trends that can be seen are weak and have a small extent (and are therefore less reliable). They do not show any link between the wind field and the GW kinetic energy.

## 4.2 Collm 52° N, 15° O

The measured and simulated climatologies in Collm show a very similar pattern as the climatologies in Kiruna and are not shown here.

The calculated trends for different properties for Collm are illustrated in figure 4. Figure 4a shows the linear trend of the measured zonal wind over Collm. With the exception of the strong positive trends in January, there are only trends in very limited regions, which are not very reliable and will not be discussed any further.

The positive trend in January can also be found in the meridional monthly-mean winds (see figure 4b). However, the meridional wind shows additional more pronounced trends, which expand over multiple months and hence are more reliable. These trends occur from May to August in around 100 km altitude as a strong negative trend and from June to August in 78 km to 86 km altitude as a strong positive trend. At some points, the p-values are lower than 0.01. In the long term, these trends will shift the summer-southerly winds toward higher altitudes.

In contrast to the weak trends of the zonal wind, the meridional trends correspond very well to trends in the GW kinetic energy, presented in figure 4c. The increase in GW activity occurs in the same region where the absolute value of the meridional wind increases (the wind becomes more negative). Vice versa, the region with a decrease of the total meridional wind (the wind becomes less negative) also shows a decline in GW kinetic energy.

The simulations by GAIA fail to reproduce any of these trends. The simulated meridional wind trends can be seen in figure 4d

### 4.3 Tavistock 43° N, 81° W

The third station considered here is the CMA station in Tavistock, Ontario. The climatologies are again roughly in accordance with the theory and are not shown here. The climatologies produced by GAIA are again reasonably close to observations, with similar problems as described in section 4.1. They are not provided here.

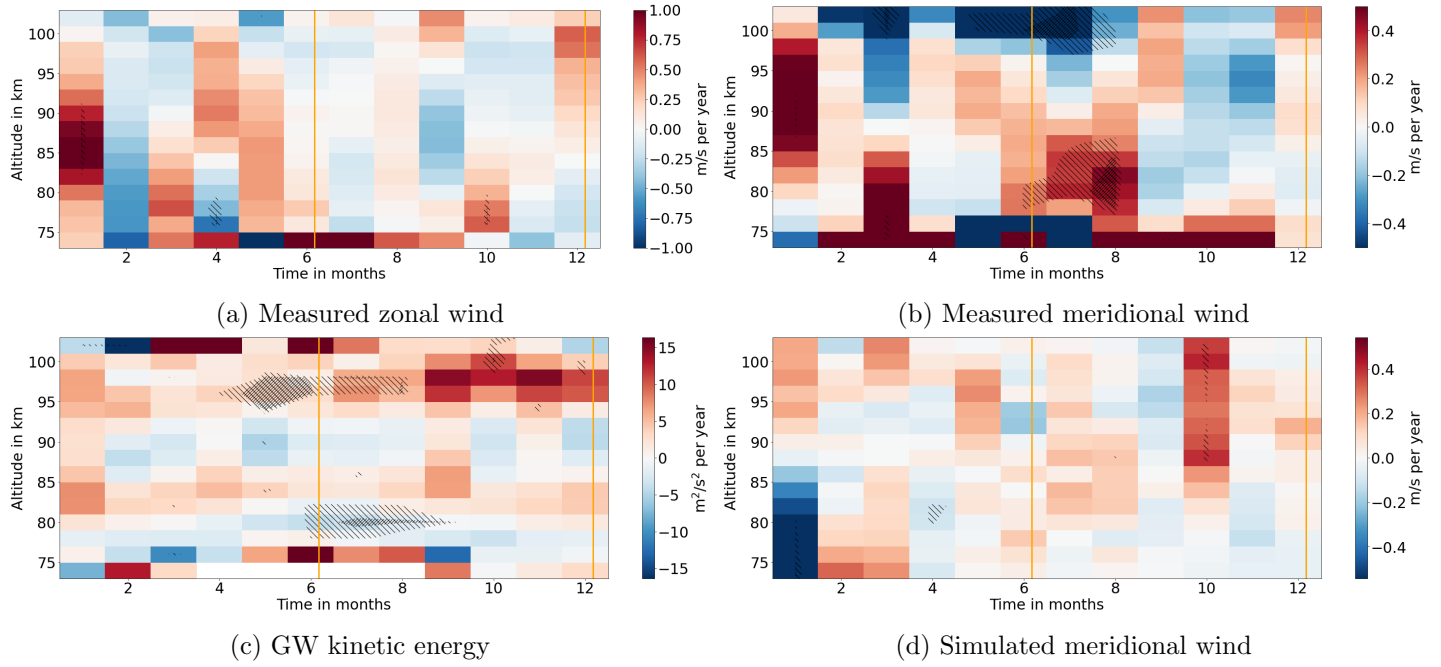


Figure 4: Linear trends of measured and simulated monthly-mean winds as well as the measured trend of the monthly-mean GW kinetic energy in Collm.

However, the measured and simulated trends are shown in figure 5. While the measured zonal wind (figure 5a) does not show any larger significant trends, the simulations (figure 5c) do in fact show a pattern of significant trends in the zonal wind. In May and June, the simulations show a significant negative trend in zonal wind speed in altitudes above 95 km. After the solstice, in July there is again a negative trend, this time between 75 km and 85 km.

The situation in the meridional wind component is reversed. While the measured meridional winds (figure 5b) do show significant trends, GAIA does not show significant trends. The most pronounced trend in the observation can be seen in May between roughly 85 km to 95 km. Located in May, right before the summer solstice, this positive trend will lead to a later and more rapid begin of the summer-southward wind. In the long term, this will lead to a “sharpening” of the transition between winter and summer circulation.

The GW kinetic energy is not shown here, as there are only very weak, hardly significant, trends visible.

#### 4.4 Rio Grande 53° S, 67° W

Figure 6 shows the measured climatologies of the meridional wind and the GW kinetic energy for Rio Grande. The climatology of the zonal wind is again in good agreement with the theory for the southern hemisphere and is not shown. The trends of the zonal wind in Rio Grande are also not discussed here as there was no hint towards a connection of those trends to GW activity. Instead, the focus lies on the trends of the meridional wind and GW kinetic energy.

The climatologies of the meridional wind and the GW kinetic energy in Rio Grande are shown in figures 6a and 6b. The meridional wind has its absolute maximum during the northern hemisphere winter where there is a strong northward flow. However, there is also a distinct minimum during May and April in around 100 km altitude. This small minimum is not explained by the basic theory for the zonal-mean wind. The climatology of the GW kinetic energy shows a maximum in the same region as well. In May and April, above 100 km by far the most GW kinetic energy of the year is produced.

It is this very same region that also shows a significant trend in the monthly-mean wind and, to a smaller extent, also a significant trend in the GW kinetic energy. Both of these trends are absolute-negative as the positive trend in the meridional has to be related to the negative winds in the climatology. The trends in the GW kinetic energy are only in a small region, but they are quite strong in the whole region and are therefore likely to be somewhat reliable nonetheless.

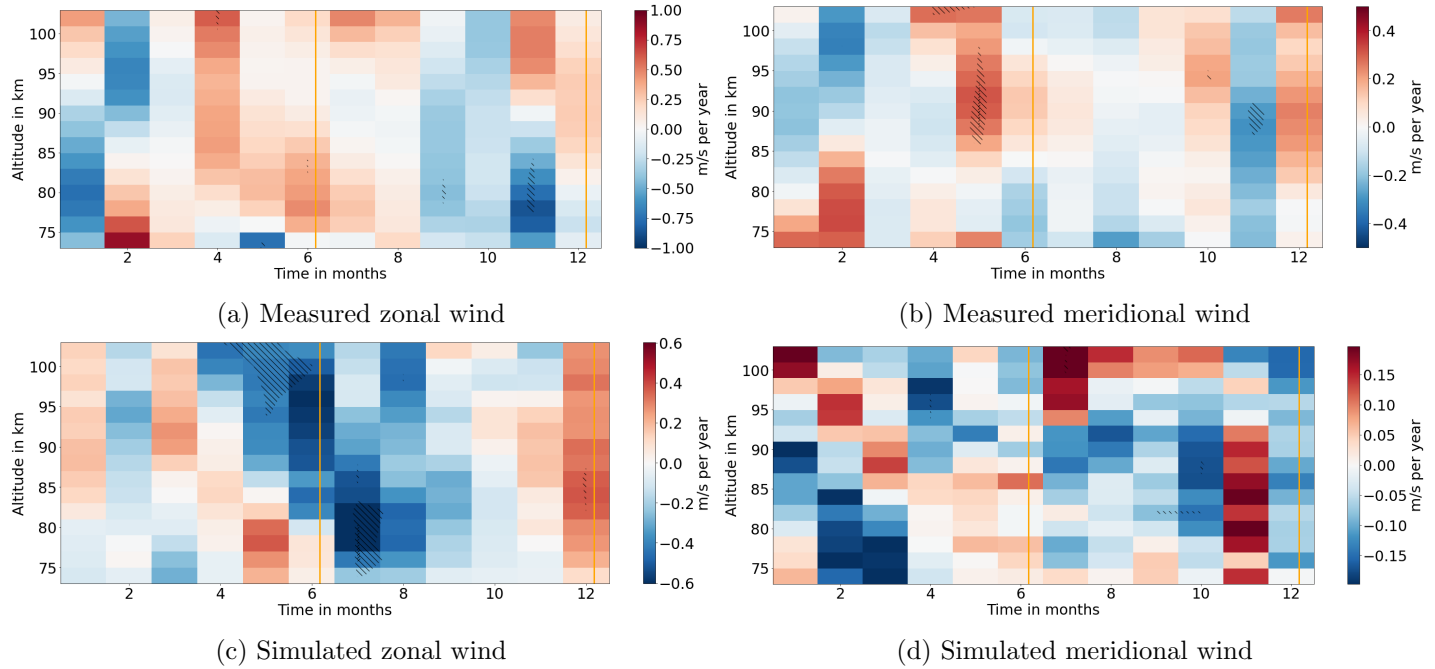


Figure 5: Linear trends of the monthly-mean zonal and meridional wind for the CMA station in Tavistock

## 4.5 Davis-Station $68^\circ$ S, $77^\circ$ O

The most southern station considered for this project is located at Davis-Station in Antarctica. Figure 7 shows the measured and simulated zonal wind trends. The following discussion is in large parts also valid for the meridional wind, although the plots for the meridional wind component will not be shown nor specifically analysed here.

The linear trends which were calculated from the observations (figure 7a) and the simulations (figure 7b) fit outstandingly well in comparison to the other stations. Especially the strong positive trends in November and December, although not significant, are very well reproduced by GAIA. The kinetic energy of the GWs (figure 7c) is generally low during the whole year and does not show any significant trend at all.

The very good performance by GAIA at the Davis station becomes even clearer in figure 7d, which shows the measured and simulated monthly-mean zonal wind year by year. GAIA was able to simulate the inter-annual changes of the wind with high accuracy and with only a small offset. The linear trends are marked in this figure as lines in orange (for the meteor radar) and red (for GAIA). This figure also underlines the importance of longer time series, as the linear trends show big differences in slope despite the great similarities in the data.

## 5 Discussion

### 5.1 The stations

The measured climatologies were found to be in good agreement with the theory presented in section 1.1. The simulated climatologies were at least able to reproduce the basic pattern, but failed in simulating smaller details and also did not feature the wind reversal during the summer circulation. The driving force of this wind reversal is believed to be GW activity. An underestimation of the GWs by GAIA could be an explanation for this deviation from the observations.

Many stations were found to feature significant long-term trends. Trends in the zonal wind shows a corresponding trend in the GW activity less often than trends in the meridional component. This was the case in Collm and in Rio Grande. However, there is no case where zonal wind trends but not meridional wind trends correspond to trends in GWs. This phenomenon might be based on the fact that the meridional wind is based on the disturbance of the zonal wind. It therefore seems plausible that the meridional circulation is more sensitive toward changes in the GW activity. It is also important to note that the direction of the implications is not trivial, since a change in the wind also leads to a change in GW activity due to changed filtering.

Kiruna and Davis show less GW activity and less significant trends than the mid-latitude stations. The trends

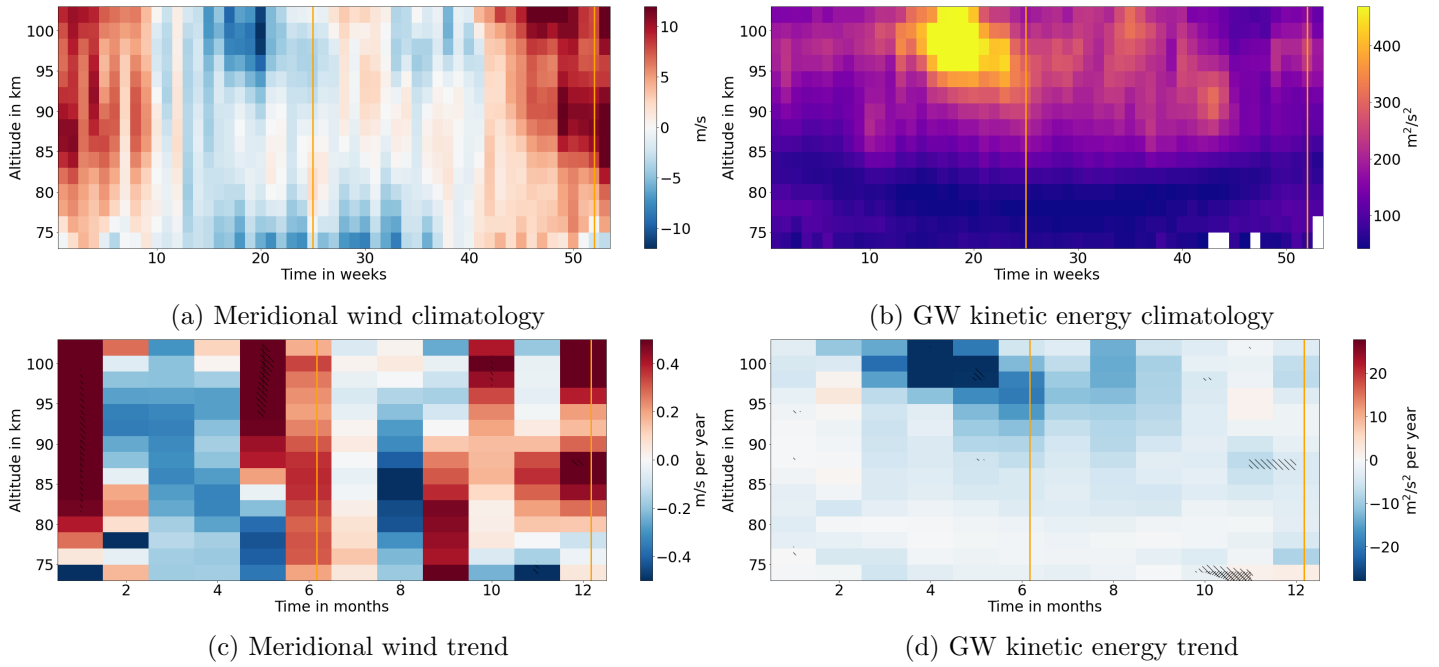


Figure 6: Measured meridional winds and GW kinetic energy climatologies and trends for Rio Grande

in the wind field do not seem to be related to GW changes at these two stations. Other sources for trends should be further investigated in future studies. Baumgaertner et al. (2005), for example, did a similar investigation for Scott Base in Antarctica and discovered trends in different tides as well as in the planetary wave activity.

Locally, phenomena in the GW field seem to have a strong influence on the wind field, as can be seen from the data from Rio Grande. Here, a distinct maximum in GW kinetic energy in autumn can be seen, which is not covered by the basic theory considered for this project. The maximum of kinetic energy corresponds to a maximum in absolute meridional wind speed, which again might be a hint toward a stronger coupling between the meridional wind and the GW activity.

The better performance of the GAIA model in Davis is striking, compared to the performance at other stations. In Davis, the trends, as well as the year-to-year fluctuations, were simulated with a good accuracy and with little offset. One possible explanation could be that the trends in GWs are lower (and not significant) in Davis. However, this is also true for Kiruna, where the performance from GAIA was worse.

## 5.2 Comparison to Wilhelm et al. (2019)

Wilhelm et al. (2019) conducted a similar investigation recently. As in this project, meteor radars, an adaptive spectral filtering technique and similar time frames were used. They also used similar stations in Andenes, Juliusruh and, as with the present project, Tavistock. The data from Tavistock is the same data presented in the previous section and will be excluded here. The other two stations Andenes and Juliusruh are located not far away from Kiruna and Collm, as can be seen in figure 8. The following section aims to compare the two similar studies regarding trends and climatologies.

### 5.2.1 Comparing Andenes to Kiruna

Figure 9 shows the climatologies and trends of the zonal wind in Kiruna (figure 9a) and Andenes (figure 9b). Both climatologies feature the same structure of eastward winds during the winter and a strong wind reversal from westward to eastward winds during summer. Even small details are reproduced, such as the initial negative winds before the reversal sets in in early summer. The same is true for the climatologies of the meridional wind, which are not presented here. However, the trends in the zonal winds are highly different. The data from Andenes shows much larger areas with significant trends. However, this can at least partly be explained by the different data processing techniques. Especially striking is the trend around the summer solstice in 100 km altitude. Both Kiruna and Andenes show significant trends but with different signs here. This might indicate a high spatial dependence of the wind trends.

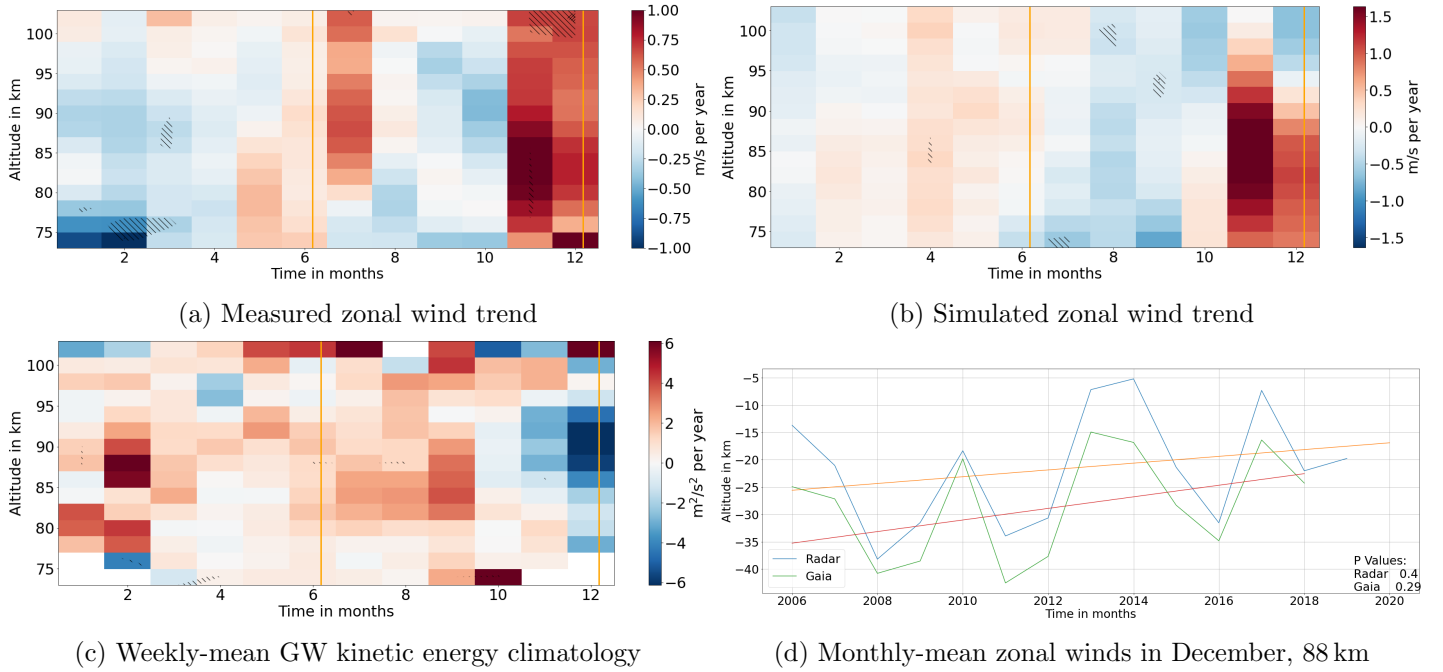


Figure 7: Monthly trends of the measured and simulated zonal mean winds, trends of GW kinetic energy and monthly-mean zonal winds in December; 88 km altitude; for Davis station

### 5.2.2 Comparing Juliusruh to Collm

Figure 10 shows meridional wind data from Collm and Juliusruh. Very similar to the situation in Kiruna/Andenes, the climatologies of Collm (figure 10a) and Juliusruh (figure 10b) are very alike. Small but distinct structures like the minimum above 100 km in August or the slightly lower wind speeds in the beginning of January, followed by a small local maximum of meridional wind speeds in all heights, are visible in both locations. The climatology of the zonal wind component is again not shown here but features great accordance between the two locations as well. Figures 10c and 10d show the trends of the meridional wind in Collm and Juliusruh. Note that the vertical frame is different. The strong significant positive trend in June, July and August in lower altitudes can be seen in both stations. The negative trend in about 100 km in Collm is outside of the frame for Juliusruh. In addition, both plots show a significant strong positive trend in January. Apart from that, Juliusruh shows a prominent negative trend in February and March, below 80 km. In this very same region, the data for Collm also shows a significant trend but with a reversed, positive sign. This might indicate that the MLT-wind field trends themselves might have a varying spatial extent. However, longer time series and uniform data processing would be necessary to further evaluate trends on such a small spatial scale.

## 6 Conclusion

This project's main aim was to investigate long-term trends in the MLT wind field over the five stations Kiruna, Collm, CMA in Tavistock, Rio Grande and Davis Station. To assess the wind MLT winds, meteor radar data that was collected between 1999 and 2019 was analysed. In addition to climatologies, a linear regression was applied to the monthly averaged data to calculate linear trends in time. After that, a hypothesis test was conducted to evaluate the significance of the calculated trends. Lastly, the climatologies and trends were compared to the results of Wilhelm et al. (2019), who conducted a similar investigation recently.

The MLT winds were found to highly variable in time and space. Besides a strong seasonal pattern, they turned out to be very variable on an inter-annual timescale. Apart from that, the main claims of this project are:

- The winds in the MLT are highly dependent on latitude, (likely) longitude, altitude and the time of year, with a strong seasonal pattern.
- Many of the stations show significant linear trends in different properties. However, these trends are not consistent between the stations in their value, sign, position in time, altitude and level of significance.

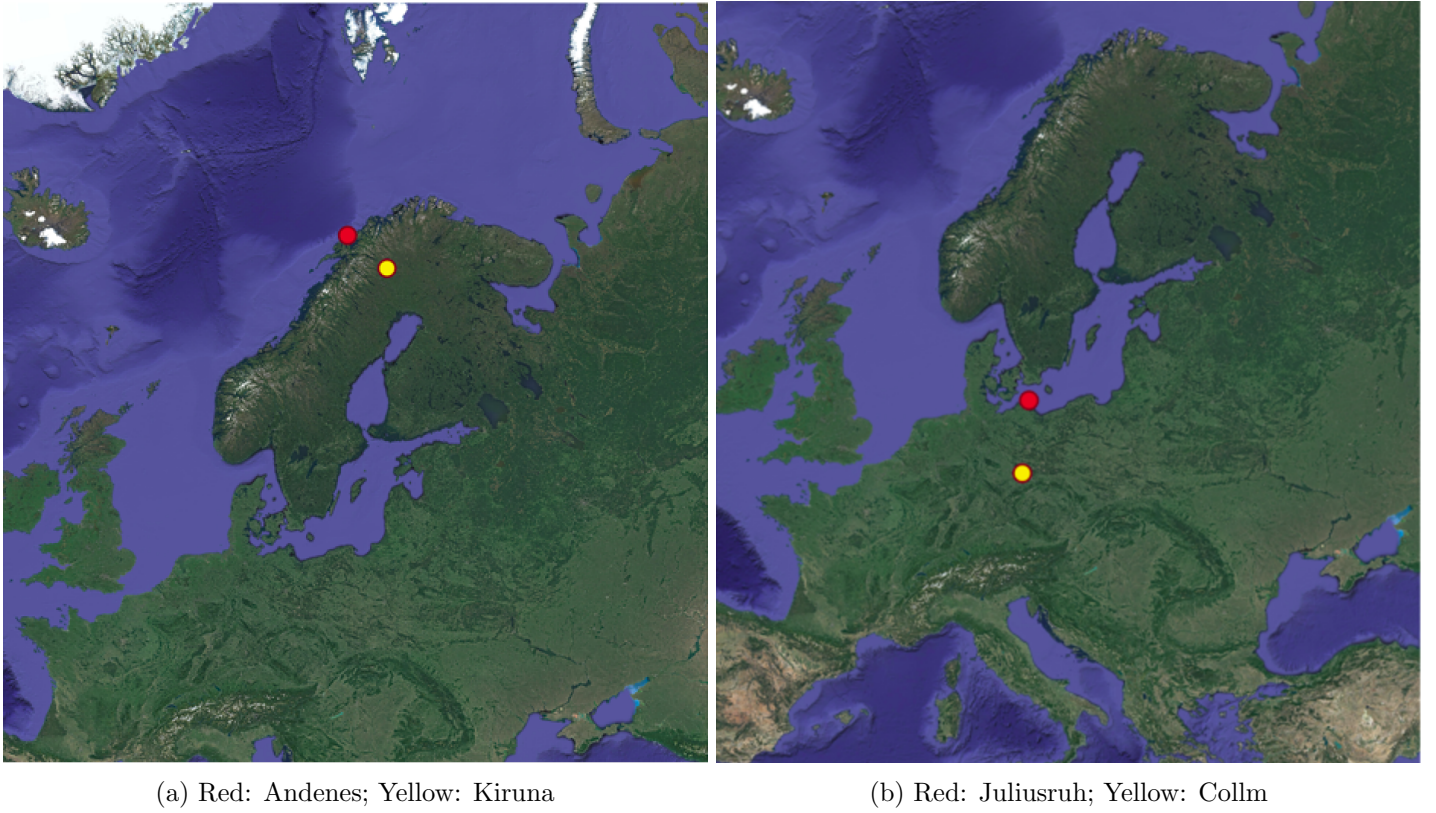


Figure 8: Maps of the stations used in this project (yellow) and by Wilhelm et al. (2019) (red)

- Some of the calculated significant trends seem to be linked to significant trends in GW activity. However, some of the trends do not show any hint to such a connection at all. In general, trends in the meridional direction and trends in lower latitudes seem to be linked more often to trends in GW activity than trends of the zonal wind component and trends of in higher latitudes.
- Mostly, GAIA was able to resolve the basic structures of the climatologies with some exceptions. Also, the calculated long-term trends differ in large parts from the measured linear trends. This is not true for Davis Station, where the model results were fairly similar to the results of the meteor radar measurements and GAIA was able to simulate the inter-annually structure in good accordance with the observations.
- The measured climatologies fit the results of Wilhelm et al. (2019) reasonably well. For the closely located stations Andenes/Kiruna and Juliusruh/Collm, even small details in the climatologies were reproduced. However, regarding the long-term trends, great differences can be seen. Possible explanations are very local effects, different data-processing techniques and different time frames.

More reliable claims could be made by using longer time series. With a maximum of 20 years, the time series used for this project are not robust against outliers as well as long-periodical cycles. There are also possible improvements in the data processing. The inclusion of the uncertainties of the measurements when calculating the trends might again make the trends more robust against errors and improve reliability. An analysis of not only the GW activity but also tidal components and planetary waves might also lead to some deeper insight. Many studies s.o. Wilhelm et al. (2019) also investigated possible links to the 11-Year solar cycle. Such a thing has not been considered for this project at all. Lastly, more stations could help to investigate the spatial structure of the MLT-dynamics as well as the spatial distribution of linear trends. Latitude-parallel stations could help to deepen the understanding of non-zonal structures, which could not be investigated in this project.

Many efforts have been made lately to investigate the dynamics of the MLT region. A deeper understanding of the long-term trends of the middle atmosphere will help, and might even be crucial to understand the dynamics of the tropospheric climate. It is therefore both necessary and exciting to further investigate the long-term behavior of the dynamics in the MLT.

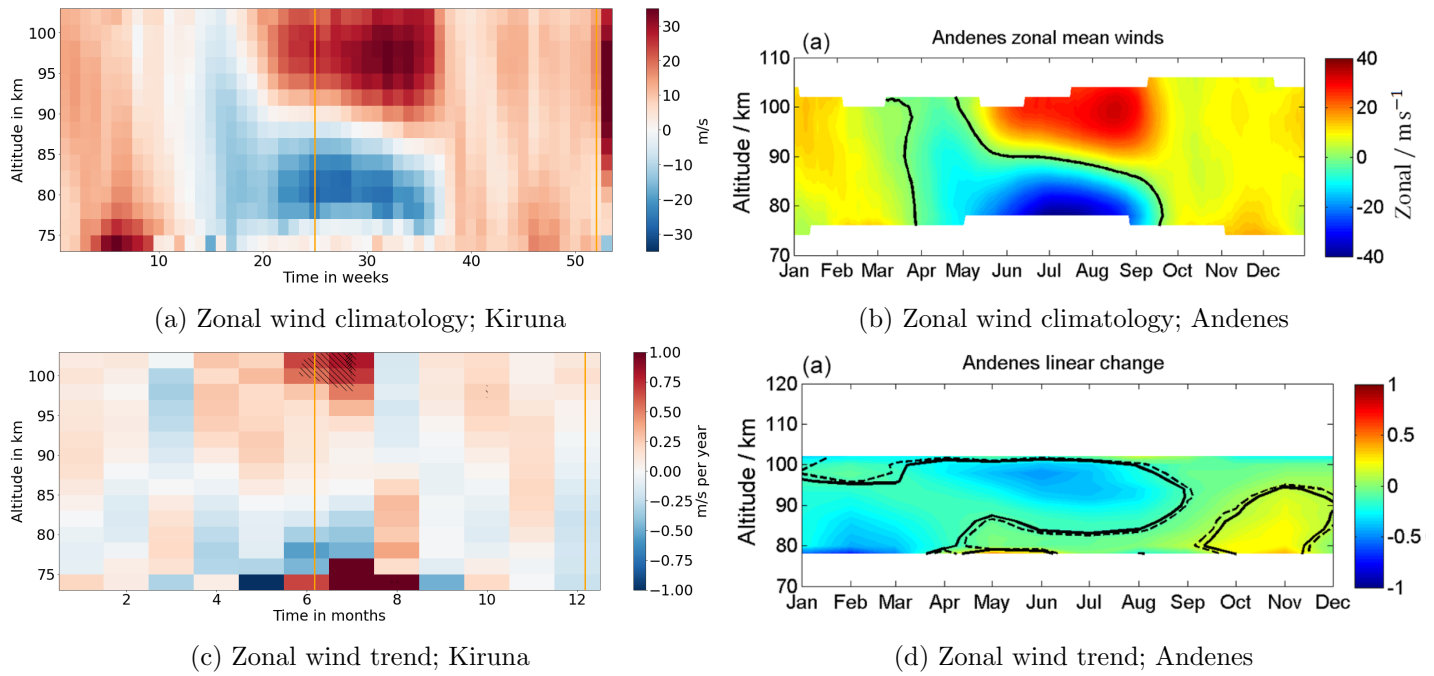


Figure 9: Measured zonal wind climatologies and trends for Kiruna and Andenes

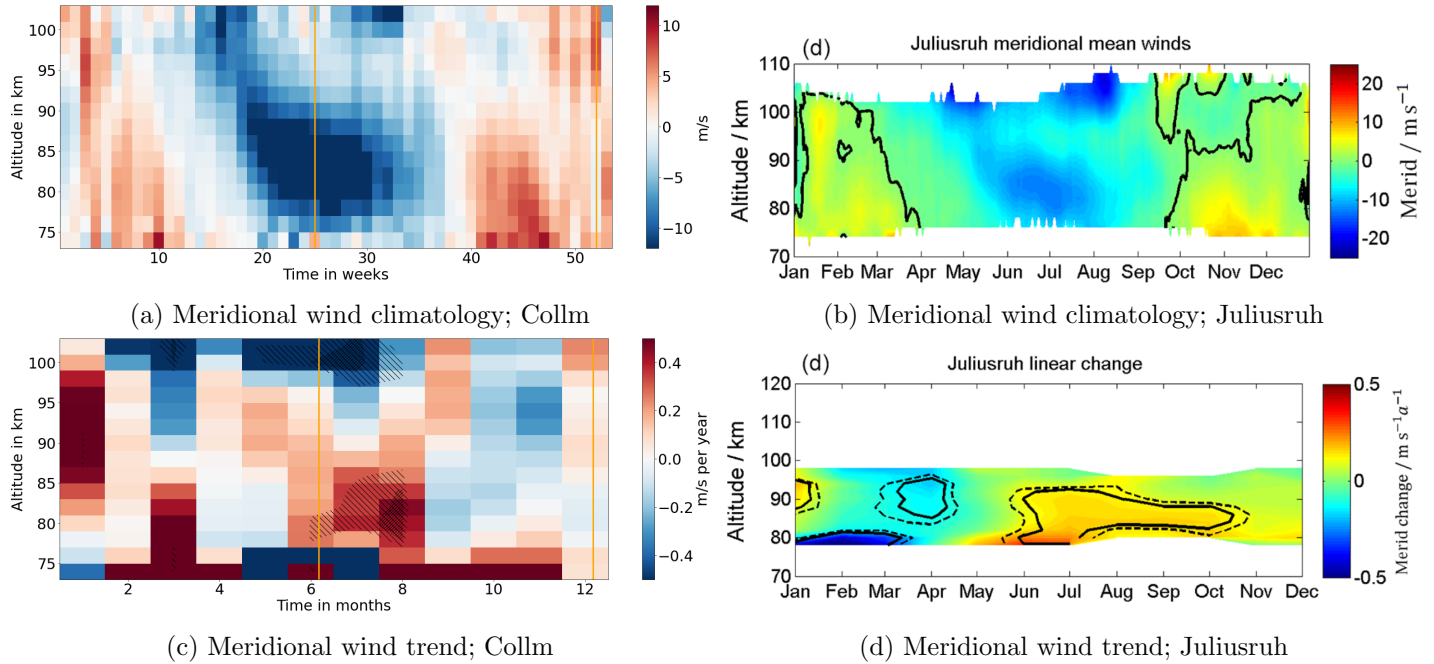


Figure 10: Measured meridional wind climatologies and trends for Collm and Juliusruh

## References

- Andrews, D. G., Leovy, C. B., and Holton, J. R. (1987). *Middle atmosphere dynamics*. Academic press.
- Baumgaertner, A., McDonald, A., Fraser, G., and Plank, G. (2005). Long-term observations of mean winds and tides in the upper mesosphere and lower thermosphere above scott base, antarctica. *J. Atmos. Sol. Terr. Phys.*, 67(16):1480–1496.
- Dowdy, A. J., Vincent, R. A., Tsutsumi, M., Igarashi, K., Murayama, Y., Singer, W., and Murphy, D. J. (2007). Polar mesosphere and lower thermosphere dynamics: 1. mean wind and gravity wave climatologies. *J. Geophys. Res. D: Atmos.*, 112(D17).
- Fritts, D. C. and Alexander, M. J. (2003). Gravity wave dynamics and effects in the middle atmosphere. *Rev. Geophys.*, 41(1).
- Geller, M. A. and Gong, J. (2010). Gravity wave kinetic, potential, and vertical fluctuation energies as indicators of different frequency gravity waves. *J. Geophys. Res. D: Atmos.*, 115(D11).
- Holton, J. R. (2012). An introduction to dynamic meteorology, 5th edition. *Am. J. Phys.*, 41(5):752–754.
- Jacobi, C., Hoffmann, P., Liu, R., Merzlyakov, E., Portnyagin, Y. I., Manson, A., and Meek, C. (2012). Long-term trends, their changes, and interannual variability of northern hemisphere midlatitude mlt winds. *J. Atmos. Sol. Terr. Phys.*, 75:81–91.
- Jacobi, C., Lange, M., Kürschner, D., Manson, A., and Meek, C. (2001). A long-term comparison of saskatoon mf radar and collm lf d1 mesosphere-lower thermosphere wind measurements. *Phys. Chem. Earth Part C*, 26(6):419–424.
- Jacobi, C., Portnyagin, Y. I., Merzlyakov, E., Solovjova, T., Makarov, N., and Kürschner, D. (2005). A long-term comparison of mesopause region wind measurements over eastern and central europe. *J. Atmos. Terr. Phys.*, 67(3):229–240.
- Palo, S. (2007). Meteors, meteor radar and mesospheric winds. In *CEDAR Workshop. Santa Fe*.
- Portnyagin, Y. I., Merzlyakov, E., Solovjova, T., Jacobi, C., Kürschner, D., Manson, A., and Meek, C. (2006). Long-term trends and year-to-year variability of mid-latitude mesosphere/lower thermosphere winds. *J. Atmos. Sol. Terr. Phys.*, 68(17):1890–1901.

- Rind, D. and Lacis, A. (1993). The role of the stratosphere in climate change. *Surv. Geophys.*, 14(2):133–165.
- Thomas, G. (1996). Global change in the mesosphere-lower thermosphere region: has it already arrived? *J. Atmos. Terr. Phys.*, 58(14):1629–1656.
- Wilhelm, S., Stober, G., and Brown, P. (2019). Climatologies and long-term changes in mesospheric wind and wave measurements based on radar observations at high and mid latitudes. In *Ann. Geophys.*, volume 37, pages 851–875. Copernicus GmbH.
- Wilhelm, S., Stober, G., and Chau, J. L. (2017). A comparison of 11-year mesospheric and lower thermospheric winds determined by meteor and mf radar at 69 n. In *Ann. Geophys.*, volume 35, pages 893–906. Copernicus GmbH.